

$3Q_y$ RESONANCE CORRECTION AT LHC INJECTION

E.H. Maclean, K. Paraschou, R. Tomás, T. Persson, S. Horney, M. Le Garrec, J. Dilly,
F.S. Carlier, V. Ferrentino, W.V. Goethem, S. Kostoglou, F. Soubelet, K. Skoufaris
CERN, Geneva, Switzerland

Abstract

Compensation of the $3Q_y$ resonance at injection energy in the LHC is of significant interest, given its potential to degrade the lifetime of high-intensity beams. In the absence of dedicated corrector circuits for the $3Q_y$, compensation of each beam at low energy, an alternative approach is needed. Using skew-sextupoles in the four common experimental insertions it has been possible to develop a scheme to independently control the $3Q_y$ resonance of the two LHC beams. Beam-based measurements and corrections of the $3Q_y$ resonance at injection were performed, with beneficial impacts on lifetime and emittance growth.

$3Q_y$ MEASUREMENT VIA FORCED RDT

The $3Q_y$ resonance can have a detrimental impact on LHC operation at 450 GeV: for example, during the 2023 ion run shifting working point (WP) from $Q_y = 0.310$ to $Q_y = 0.306$ improved beam-lifetime by a factor 4.

During proton operation, the role of $3Q_y$ can be somewhat mitigated by lowering Q_y , at the cost of increasing detrimental impacts of Landau octupole (MO) driven resonances $4Q_x$ and $2Q_x - 2Q_y$. None-the-less, in simulation the $3Q_y$ resonance has still been linked with potential for unwanted emittance growth and tail generation [1, 2], and in measured loss maps with breaking of collimator hierarchy [3–6]. In future runs, changes to operational polarities of the MO will increase relevance of $3Q_y$, such configurations demanding WPs closer to the resonance.

The $3Q_y$ resonance has been studied in the LHC via resonance driving terms [7–10] (RDT) measured via forced-oscillations with an AC-dipole [11–13] (ACD). While conventional RDT measurements with kicked beams have been used to good effect in many machines [9, 14–18], forced oscillations offer considerable advantages. Forced oscillations do not decohere, allowing spectral analysis on the full 6600 turn ACD excitation (compared to typically a few hundreds of turns for LHC single kicks), and removing the need to correct RDT measurements for distortion by decoherence [9]. Figure 1 (right) shows the measured spectra from an ACD kick, the component at $-2 \times Q_{y,AC}$ relating to the $3Q_y$ resonance being clearly visible.

The Forced-RDT f'_{0030} characterizes the perturbation of forced oscillations by the resonance $Q_{y,AC} + 2Q_y$ [19], which is a proxy of the free $3Q_y$ in forced motion. This is measured via the amplitude of the frequency component which appears at $-2Q_{y,AC}$ in the vertical turn-by-turn (TbT) data. Figure 2 compares the measured f'_{0030} in LHCB1 at 450 GeV during dedicated tests in 2022, to predictions of the LHC model.

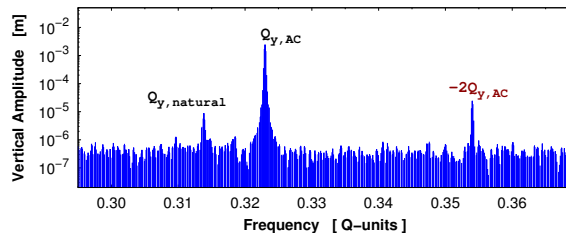


Figure 1: Example of spectra from an ACD excitation.

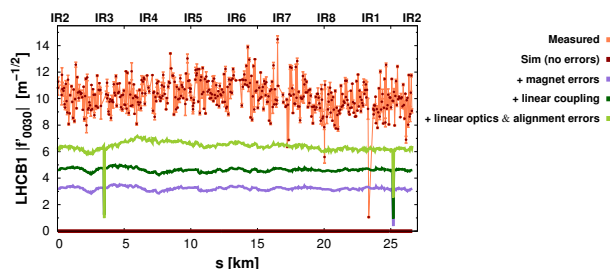


Figure 2: Measured/model f'_{0030} of LHCB1 at 450 GeV.

The bare LHC lattice (Fig. 2, red) shows negligible $3Q_y$ strength. Introducing nonlinear errors based on magnetic measurements [20, 21] increases f'_{0030} (Fig. 2, purple), dominated by the skew-sextupole component of the main bends. A small increase in $3Q_y$, from matching linear coupling to the approximate amplitude and phase seen during the measurements is shown in Fig. 2 (dark green). Finally, Fig. 2 (light green) shows the prediction of the best-knowledge LHC model, including all known magnetic and alignment errors, plus effective models approximating observed linear coupling and optics distortions at the time of the measurement. Even with this model a large discrepancy exists with measured $3Q_y$ strengths. Consequently model-based optimization, as proved effective for normal sextupole resonances [22], is not possible and a beam-based approach is required.

DA simulations used to inform LHC operation do not normally include sources of nonlinear errors (primarily studying roles of chromaticity and MO tune spread). To assess the relevance of the observed $3Q_y$ effective models were generated, artificially introducing skew-sextupole sources to match the magnitude of f'_{0030} . Figure 3 compares the standard LHC DA prediction for 2022 operation in Xsuite, to those including the effective $3Q_y$. A clear reduction of the good DA region is visible. Degradations were similarly observed in 20×10^3 turn in PTC (*Polymorphic Tracking Code*) Frequency Map Analysis [23], while simulations of

the 2022 operational configuration in Xsuite, including e-cloud effects, also showed an increase to emittance growth in the 5 – 10 % range upon including the effective $3Q_y$ [2]. Correction of the resonance at LHC injection is therefore well motivated.

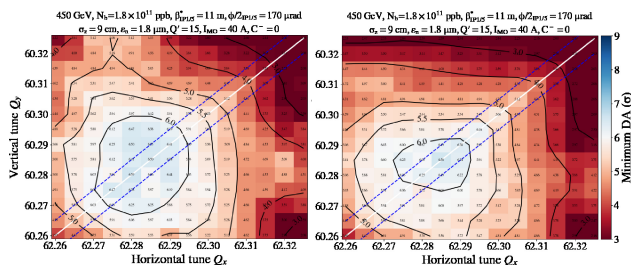


Figure 3: LHCb1 DA simulations in Xtrack, for 2022 operation at 450 GeV, for the standard LHC simulation setup (left), and including an effective model of f'_{0030} (right).

SINGLE BEAM CORRECTION TESTS

The LHC was designed without correctors for control of $3Q_y$ at 450 GeV: skew-sextupole magnets in the arcs being purposefully arranged to control chromatic coupling without perturbing $3Q_y$. The only other skew-sextupoles are seven correctors in the experimental insertions, for local compensation of nonlinearities at top energy [24]. While these IR-skew-sextupoles (MCSSX) have sufficient strength to help control $3Q_y$ at 450 GeV [25], they are located in the common aperture region of the collider [26], and thus simultaneously influence both beams.

Initial studies focusing on single-beam $3Q_y$ compensation, were performed during dedicated beam-tests in 2022 [23]. Figure 4 shows the LHCb1 model's f'_{0030} response of individual MCSSX to a powering change of $\Delta K_3 = +0.5 \text{ m}^{-3}$ (at arbitrarily selected BPM.30R1.B1). Following initial measurements of the f'_{0030} and noting the highly orthogonal responses of the MCSSX left of IP8 (LHCb), with those right of IP1 (ATLAS) and IP5 (CMS), these three correctors were powered to minimize the observed $3Q_y$ of LHCb1. Figure 5 shows the measured f'_{0030} of both beams before (red/orange) and after (dark/light blue) application of the optimal settings found for LHCb1. Figure 5 encapsulates the challenge of correcting $3Q_y$ via common aperture MCSSX. In correcting LHCb1, LHCb2 has been substantially degraded. Several studies were performed to confirm with operational MO and chromaticity that variation of RDT amplitude translated to changes in beam-lifetime. In Fig. 6 (left) vertical tune was increased to $Q_y = 0.33$ resulting in low beam-lifetime ($\sim 0.6 \text{ h}$). On application of the LHCb1 correction shown in Fig. 5 lifetime was observed to double. In Fig. 6 (right) the lifetime of LHCb2, even while much further from the resonance ($Q_y = 0.31$), showed clear degradation corresponding to the increase of $|f'_{0030}|$ as the LHCb1 correction was applied. Similar RDT and lifetime results were obtained for optimization of LHCb2 [23]. While not useful for operation, these single-beam tests confirm the basic premise that

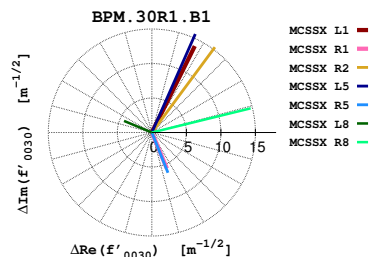


Figure 4: f'_{0030} response of LHCb1 to MCSSX in 2022.

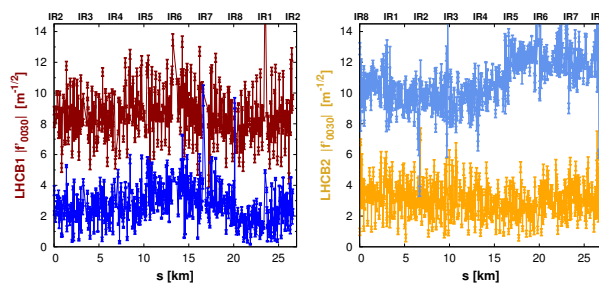


Figure 5: Measured $|f'_{0030}|$ of LHCb1 (left) and LHCb2 (right), before and after application of the best correction found for LHCb1.

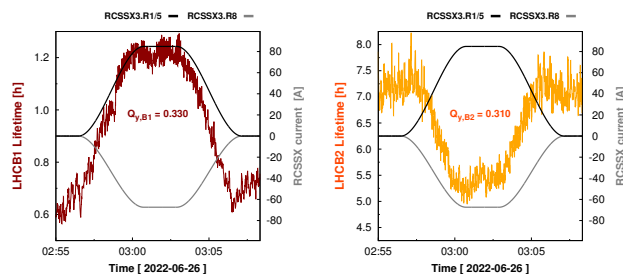


Figure 6: Lifetime of LHCb1 (left) and LHCb2 (right) on application of LHCb1 optimized $3Q_y$ correction.

globally optimizing f'_{0030} using the MCSSX translated to a lifetime improvement.

DUAL BEAM COMPENSATION SCHEME

In 2023, a new injection optics was deployed [27]. Figure 7 (top) shows the LHCb1 and LHCb2 MCSSX response at BPM.30R1. By combining the circuits, several knobs were identified allowing independent control of the beams, Fig. 7 (bottom). For example, powering MCSSX left of IP8 plus MCSSX right of IP2 (at 30 % of L8 strength) generates a large shift in LHCb2, while self-cancelling in LHCb1 (Fig. 7, bottom, grey). Relatively orthogonal knobs were identified in LHCb2, though LHCb1 was more restricted in phase. Approximate orthogonality and independence was preserved around the ring.

The new optics (coincidentally) gave a substantial change to $3Q_y$: degrading LHCb2 but improving LHCb1. In dedicated beam-tests a simple response matrix correction could compensate the RDT, shown in Fig. 8. The large RDT in Beam2 was considerably reduced, while the already small Beam1 was slightly improved.

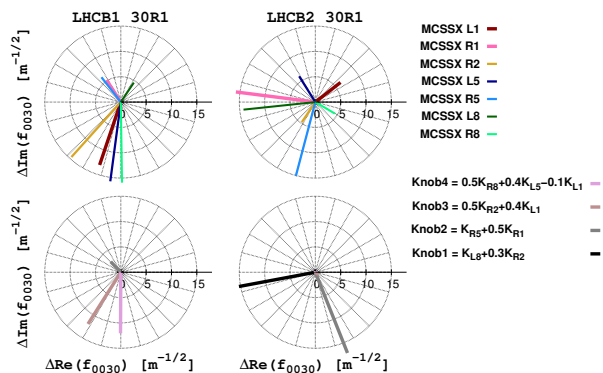


Figure 7: LHC B1 (left) and LHC B2 (right) f'_{0030} response to MCSSX for 2023 LHC injection optics (top) and independent beam knobs (bottom).

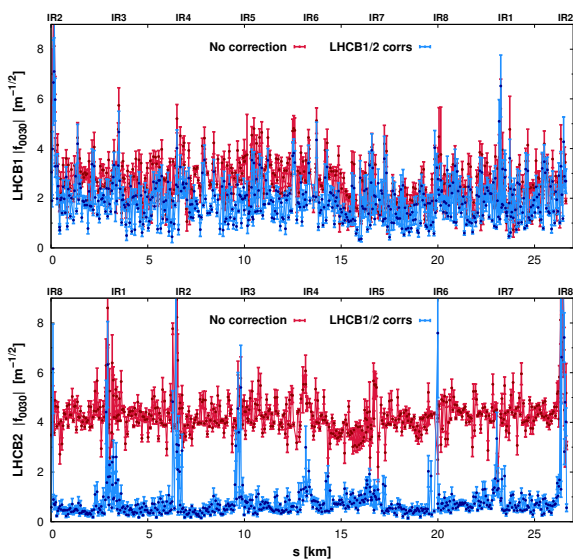


Figure 8: $3Q_y$ correction of 2023 LHC injection optics.

The corrections were employed during e-cloud beam studies to examine the impact on LHC trains. Figure 9 shows surviving beam-intensity along several trains in LHC B2, for differing Q_y . As the WP approaches $3Q_y$, a pattern of losses appears, as e-cloud Q -spread induces higher losses on the resonance. After correction, the losses were substantially reduced. Separate tests also demonstrated that correction yielded improvements to transmission of high-intensity bunches on resonance crossing [2]. A reduction in emittance growth was also observed for working points approaching $3Q_y$. Figure 10 compares emittance measurements at the end of the train for $Q_y = 0.29$ (blue) and $Q_y = 0.32$ (red). Before correction (left, red) substantial emittance growth was observed, after correction (right, red) this was significantly reduced. The $3Q_y$ correction scheme was used for 2023 LHC operation. Following optics changes in 2024, the exercise was repeated, and once again operational corrections of both beams were found.

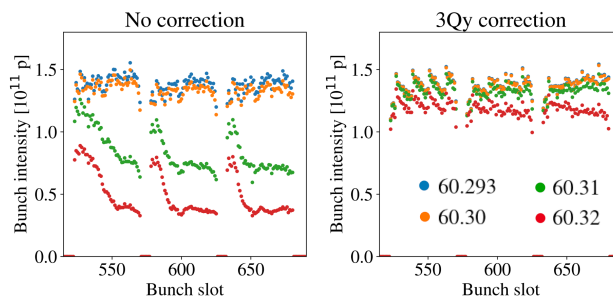


Figure 9: Surviving intensity vs working point along LHC bunch trains before (left) and after (right) $3Q_y$ correction.

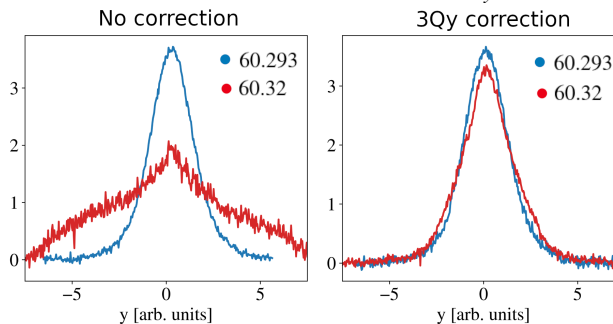


Figure 10: Vertical beam profile at end of a train before (left) and after (right) $3Q_y$ correction, for working points $Q_y = 0.29$ (blue) and $Q_y = 0.32$ (red).

CONCLUSIONS

Although the LHC does not have any correctors intended for $3Q_y$ compensation at injection, it has been possible to co-opt common aperture IR-skew-sextupoles in the experimental insertions to achieve meaningful reductions in forced-RDT strength. In single-beam tests this was clearly associated with improvements in lifetime of low-intensity bunches. By using combinations of the MCSSX magnets to define independent knobs for the two beams, operational corrections have been achieved. These exhibited improvements to losses and emittance growth with nominal beams when approaching the resonance, increasing the viable WP range for LHC operation. This will be of particular relevance to future operation with reversed polarity Landau octupoles in the LHC, where WP closer to the $3Q_y$ resonance than today is required.

ACKNOWLEDGMENTS

Many thanks go to the LHC EIC's and operations team for their support of the experimental studies presented here.

REFERENCES

- [1] E.H. Maclean *et al.* "A mechanism for emittance growth based on non-linear islands in the LHC", in *Proc. IPAC'21*, Campinas, Brazil, 2021, THPAB169. <https://accelconf.web.cern.ch/ipac2021/papers/thpab169.pdf>
- [2] K. Paraschou, "Proposal for changes to the injection optics", presented at CERN LHC Beam Operation Committee (LBOC), Mar. 2023. <https://indico.cern.ch/event/1261566/>.

- [3] R. Tomás, A. Calia, M. D'Andrea, L. Deniau, D. Jacquet *et al.*, "Mitigation of losses at injection protection devices in the CERN LHC", in *Proc. of IPAC'23*, Venice, Italy, 2023. <https://accelconf.web.cern.ch/ipac2023/pdf/MOPL019.pdf>
- [4] F. V. D. Veken, "Collimation commissioning", presented at the CERN Joint Accelerator Performance Workshop, Dec. 2022. <https://indico.cern.ch/event/1194548>
- [5] M. D'Andrea, "Follow up of action: Refined analysis of TDIS loss maps", presented at the CERN NDC section meeting, Dec. 2022. <https://indico.cern.ch/event/1225695/>
- [6] M. D'Andrea, "Update on TDIS losses", presented at the CERN NDC section meeting, Nov. 2022. <https://indico.cern.ch/event/1219705/>
- [7] A. Bazanni, E. Todesco, and G. Turchetti, "A normal form approach to the theory of nonlinear betatronic motion", CERN, Geneva, Switzerland, Rep. CERN-94-02, 1994. <http://cds.cern.ch/record/262179>
- [8] R. Bartolini and F. Schmidt, "Normal form via tracking or beam data", LHC-Project-Report-132, vol. 59, pp. 93-106, 1998. <http://cds.cern.ch/record/333077>
- [9] R. Tomás, "Direct Measurement of Resonance Driving Terms in the Super Proton Synchrotron (SPS) of CERN using Beam Position Monitors", Ph.D. dissertation, Universitat de València, 2003. <http://cds.cern.ch/record/615164>
- [10] A. Franchi, "Studies and Measurements of Linear Coupling and Nonlinearities in Hadron Circular Accelerators", Ph.D. dissertation, Universität Frankfurt, 2006.
- [11] J. Serrano and M. Cattin, *The LHC AC Dipole system: an introduction*, Tech. Rep., CERN-BE-Note-2010-014, 2010.. <http://cds.cern.ch/record/1263248>
- [12] E. Carlier, L. Ducimetiere, and E. Vossenberg, "A Kicker Pulse Generator for Measurement of the Tune and Dynamic Aperture in the LHC", in *Conference record of the twenty seventh international power modulator symposium*, 2006. doi:10.1109/MODSYM.2006.365284
- [13] R. Barlow, E. Carlier, J. Pianfetti, V. Senaj, and M. Cattin, "Control of the MKQA tuning and aperture kickers of the LHC", Tech. Rep., CERN-TE-Note-2010-001, 2010. <https://cds.cern.ch/record/1232062?ln>
- [14] A. Franchi, R. Tomás, and F. Schmidt, "Magnet strength measurement in circular accelerators from beam position monitor data", *Phys. Rev. Spec. Top. Accel Beams*, vol. 10, no. 074001, 2007. doi:10.1103/PhysRevSTAB.10.074001
- [15] M. Carla *et al.*, "Status of the beam-based measurement of the skew-sextupolar component of the radio frequency field of a HL-LHC-type crab-cavity", in *Proc. of IPAC 23*, Venice, Italy, May 2023, pp. 504–507. doi:10.18429/JACoW-IPAC2023-MOPL001
- [16] M. Carla, A. Alekou, H. Bartosik, and L.R. Carver, "Beam-based measurements of the skew-sextupolar component of the radio frequency field of a HL-LHC-type crab-cavity", Tech. Rep., CERN-ACC-2020-0024, 2020. <https://cds.cern.ch/record/2715376>
- [17] W. Fischer, R. Tomas, and F. Schmidt, "Measurement of sextupolar resonance driving terms in RHIC", in *Proc. of PAC 2003*, 2003, MOPL001. <https://accelconf.web.cern.ch/p03/PAPERS/WPAB080.pdf>
- [18] A. Franchi, L. Farvacque, F. Ewald, G. Le Bec, and K.B. Scheidt, "First simultaneous measurement of sextupolar and octupolar resonance driving terms in a circular accelerator from turn-by-turn beam position monitor data", *Phys. Rev. Spec. Top. Accel Beams*, vol. 17, no. 074001, 2014. doi:10.1103/PhysRevSTAB.17.074001
- [19] R. Tomás, "Normal form of particle motion under the influence of an ac dipole", *Phys. Rev. Spec. Top. Accel Beams*, vol. 5, no. 054001, 2002. doi:10.1103/PhysRevSTAB.5.054001
- [20] WISE, <http://wise.web.cern.ch/WISE/>
- [21] P. Hagen, *WISE - user guide and implementation notes*, <http://wise.web.cern.ch/WISE/Doc/lhc-project-report-wise.pdf>
- [22] S.J. Horney, E.H. Maclean, P. Burrows, F. Carlier, L. Deniau *et al.*, "Sextupole RDTs in the LHC at injection and in the ramp", in *Proc. IPAC'24*, Nashville, TN, USA, May 2024, pp. 71–74. doi:10.18429/JACoW-IPAC2024-MOPC13
- [23] E.H. Maclean *et al.*, *Report from LHC MD6904: 3Qy correction at 450 GeV*, Tech. Rep., 2024, CERN technical report, awaiting publication.
- [24] E.H. Maclean *et al.*, "New approach to LHC optics commissioning for the nonlinear era", *Phys. Rev. Accel. Beams*, vol. 22, no. 061004, 2019. doi:10.1103/PhysRevAccelBeams.22.061004
- [25] E. Waagaard and E.H. Maclean, "A response matrix approach to skew-sextupole correction in the LHC at injection", in *Proc. IPAC'22*, Bangkok, Thailand, Bangkok, Thailand, Jun. 2022, pp. 1987–1990. doi:10.18429/JACoW-IPAC2022-WEPOPT058
- [26] O. Bruning, S. Fartoukh, M. Giovannozzi, and T. Risselada, *Dynamic Aperture Studies for the LHC Separation Dipoles*, Tech. Rep., LHC-Project-Note-349, 2004. <https://cds.cern.ch/record/742967>
- [27] R. Tomás *et al.*, "Optics for Landau damping with minimized octupolar resonances in the LHC", *J. Instrum.*, vol. 19, 2024. doi:10.1088/1748-0221/19/05/T05010